Physical Biology

OPEN ACCESS

RECEIVED
31 May 2019

REVISED
26 July 2019

ACCEPTED FOR PUBLICATION
9 August 2019

PUBLISHED
18 September 2019

PAPER

The transmembrane protein fibrocystin/polyductin regulates cell mechanics and cell motility

Stefanie Puder[1], **Tony Fischer**[1] **and Claudia Tanja Mierke**[1,2]

Faculty of Physics and Earth Science, Peter Debye Institute of Soft Matter Physics, Biological Physics Division, University of Leipzig, Linnéstr. 5, 04103 Leipzig, Germany

[1] Contributed equally.

[2] Author to whom any correspondence should be addressed.

E-mail: claudia.mierke@uni-leipzig.de

Keywords: cell mechanics, forces, invasion, deformability, cell–cell adhesion

Supplementary material for this article is available online

Abstract

Polycystic kidney disease is a disorder that leads to fluid filled cysts that replace normal renal tubes. During the process of cellular development and in the progression of the diseases, fibrocystin can lead to impaired organ formation and even cause organ defects. Besides cellular polarity, mechanical properties play major roles in providing the optimal apical-basal or anterior–posterior symmetry within epithelial cells. A breakdown of the cell symmetry that is usually associated with mechanical property changes and it is known to be essential in many biological processes such as cell migration, polarity and pattern formation especially during development and diseases such as the autosomal recessive cystic kidney disease. Since the breakdown of the cell symmetry can be evoked by several proteins including fibrocystin, we hypothesized that cell mechanics are altered by fibrocystin. However, the effect of fibrocystin on cell migration and cellular mechanical properties is still unclear. In order to explore the function of fibrocystin on cell migration and mechanics, we analyzed fibrocystin knockdown epithelial cells in comparison to fibrocystin control cells. We found that invasiveness of fibrocystin knockdown cells into dense 3D matrices was increased and more efficient compared to control cells. Using optical cell stretching and atomic force microscopy, fibrocystin knockdown cells were more deformable and exhibited weaker cell–matrix as well as cell–cell adhesion forces, respectively. In summary, these findings show that fibrocystin knockdown cells displayed increased 3D matrix invasion through providing increased cellular deformability, decreased cell–matrix and reduced cell–cell adhesion forces.

Introduction

The epithelial morphogenesis is a highly complicated process that leads to the formation of organs by providing cellular functions such as the polarity under healthy and physiological conditions (Bryant and Mostov 2008, Wilson 2011). However, when the epithelial morphogenesis of the kidney is deregulated, diseases such as polycystic kidney disease may occur. While the biochemical, genetic and cell biological aspects of the epithelial morphogenesis are highly investigated, the influence of cell mechanics on the process of epithelial cell morphogenesis in the formation of organs such as the kidney is still less well researched.

Several proteins, including fibrocystin, have an impact on cellular symmetry, which is crucial for proper organ development. Since cell symmetry is to be controlled by the mechanical phenotype of the cells, fibrocystin appears to be involved in cell mechanics. Fibrocystin is encoded by the polycystic kidney and hepatic disease 1 (PKHD1) gene, which is one of the largest known genes of the human genome with approximately 469 kb and proposed 86 exons (Onuchic *et al* 2002). In more detail, the PKHD1 gene encodes for the transmembrane protein fibrocystin consisting of 4074 amino acids. Fibrocystin is located in the basal body of the apical domain building primary cilia of polarized epithelial cells. The fibrocystin operates in the formation of tubules and/ or ensures

the maintenance of the architecture of the lumen of the kidney. A mutation in the PKHD1 gene may be autosomal-recessive inherited leading to the autosomal recessive cystic kidney (ARPKD) with associated congenital liver fibrosis. A severe form of the cystic kidney occurs in very early age of the patient with a defect in the epithelial tube formation. As for the epithelial tube formation cellular mechanical properties and migration seem to be involved, Madin-Darby canine kidney (MDCK) cells have been chosen as a cell culture model system that were treated with PKHD1 specific siRNA in order to knock-down fibrocystin (table 1).

In more detail, MDCK cells have been successfully utilized for the analysis of epithelial cell adhesion using micro-patterned slides and it has been observed that (i) small cell-extracellular matrix adhesions and (ii) low actomyosin contractility are necessary and sufficient for the initial steps of morphogenesis in MDCK renal collecting duct epithelial cells (Rodriguez-Fraticelli *et al* 2012). MDCK cells have been analyzed on disc-shaped micropatterns with respect to the correct positioning of centrosomes and establishment of apicobasal polarity. The correct positioning and the apicobasal polarity were solely confirmed, when these cells are cultured under spatial constraints such as the confinement of epithelial cell spreading through a decreased adhesion area or when the cells were seeded onto specific extracellular matrix proteins such as laminin, which is a constituent of basal membrane surrounding organs. The confinement of cells on disc-shaped micropatterns has been demonstrated to be critical for the promotion of apicobasal polarity and hence lumen initiation within small spheroids of epithelial cells (Rodriguez-Fraticelli *et al* 2012). Moreover, confinement can alter the ciliogenesis in growth-arrested single epithelial cells (Pitaval *et al* 2010).

By inhibition of actomyosin contractility using blebbistatin, a myosin inhibitory drug, it has been reported that the positioning of the centrosome and the defects in cell morphogenesis can be restored in the absence of confinement (Pitaval *et al* 2010, Rodriguez-Fraticelli *et al* 2012). Thus, it has been proposed that both processes, such as the initiation of lumen and ciliogenesis, depend on low myosin II facilitated contractility of the cells. Based on these results it can be hypothesized that the alteration of cellular mechanical properties such as contractility impacts cellular functions. However, the effect of fibrocystin on other cellular mechanical properties such as cellular deformability, cell–cell or cellular matrix intercellular adhesion forces and cell migration in 3D microenvironments is still unclear. However, it has been found that knockdown of the PKHD1 gene in MDCK cells altered their polarization and cell spreading behavior (Rodriguez-Fraticelli *et al* 2012). In order to explore the effect of PKHD1 expression on cellular mechanical properties, we utilized a RNAi approach to transiently knockdown PKHD1 and investigated their migratory and mechanical properties.

Results

Increased motility and invasion in 3D extracellular matrices is evoked by knock-down of PKHD1 gene encoding fibrocystin

Since it is known that fibrocystin can cause a breakdown of symmetry in Kolb and Nauli (2008) and thereby increase the cell polarization (asymmetry). Besides cell polarization is connected with the motility of the cells (Watanabe *et al* 2014, Limdi *et al* 2018). In order to investigate the effect of the fibrocystin gene PKHD1 on motility and invasiveness of Madin-Darby canine kidney epithelial cells (MDCK cells), we performed invasion assays into 3D extracellular matrices consisting of collagen type I fiber networks (Fischer *et al* 2017, Kunschmann *et al* 2017, 2019, Mierke *et al* 2017) In figure 1(A), it can be representatively seen that these collagen fibers form a network of fibers and bundles with many entanglements (termed crosslinking points). To reveal whether the fibrocystin gene PKHD1 regulates invasion behavior of MDCK cells, we seeded siRNA PKHD1 (siPKHD1) and control siRNA (siCTR) treated cells on top of dense 3D extracellular matrices (collagen concentration of 1.5 g l^{-1} and 500 μm thick). After cells for 72 hours, the percentage of invaded cells (figure 1(B)) and the invasion depth (figure 1(C)) were determined. The invasiveness of siRNA PKHD1 (siPKHD1) treated cells was pronouncedly increased compared to control siRNA (siCTR) treated cells. In detail, the invasion profile of siRNA PKHD1 (siPKHD1) treated cells shows higher probabilities and 90% of all invasive cells were not found deeper than 48 μm $\pm$ 1.24 μm (figure 1(D), $n = 503\,788$ cells). In contrast, the invasion profile of control siRNA (siCTR) treated cells shows lower probabilities and 90% of invasive cells were not found deeper than 40 μm $\pm$ 0.45 μm compared to PKHD1 knock-down cells (figure 1(D), $n = 934\,251$ cells). These results indicate that the fibrocystin gene PKHD1 influences invasion behavior of MDCK cells and facilitates invasiveness into 3D extracellular matrices.

Knockdown of PKHD1 gene encoding fibrocystin increased cellular deformability

The process of cell polarization has been shown to be induced by fibrocystin and related to cell mechanics (Rodriguez-Fraticelli *et al* 2012). However, since the motility of cells is associated with cell mechanics (Mierke *et al* 2011, 2013b, 2008a, 2008b, Mierke 2013a, 2014, Blanchoin *et al* 2014) and is affected by changes in cellular deformability (equivalence for compliance or inverse of stiffness) (Fischer *et al* 2017, Kulkarni *et al* 2018), we determined the cellular deformability of these two cell types.

More precisely, the deformability of cells has been reported to be increased in highly motile cancer cells compared to less motile cancer cells of epithelial origin (Guck *et al* 2001, 2005, Fischer *et al* 2017, Meinhövel *et al* 2018). Hence, the optical cell stretcher has been

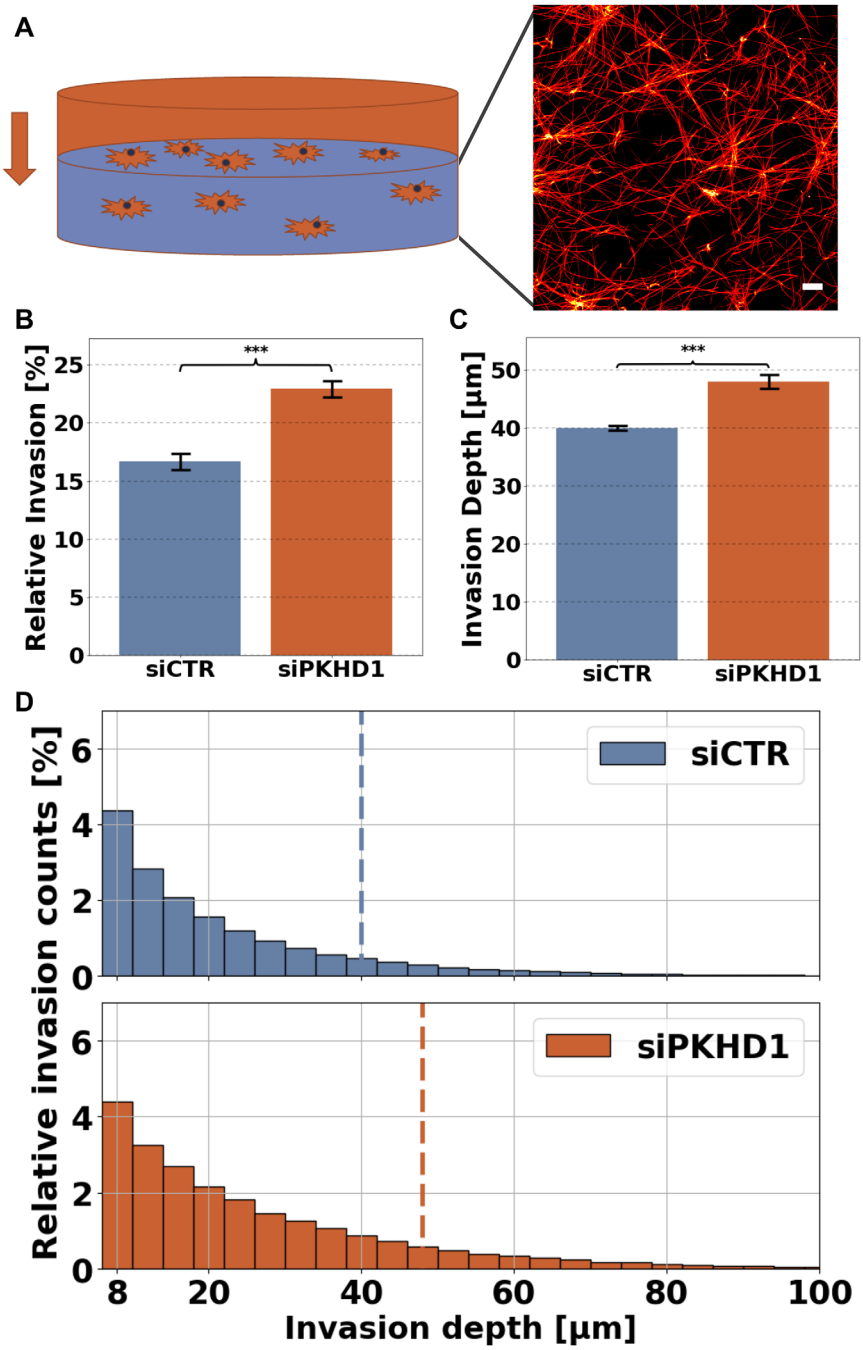

Figure 1. Cellular motility of MDCK cells treated with control siRNA (siCTR) or PKHD1 (siPKHD1) into an engineered 3D collagen microenvironment. (A) Schematic illustration of a 3D invasion assay and laser scanning confocal image of a 3D extracellular matrix stained with TAMRA. Scale bar represents 10 μm. Collagen network consisting of 1/3 collagen R type I and 2/3 collagen G type I with an end concentration of 1.5 mg ml^{-1}, pH of 7.4 and an ionic strength of 0.7. Cells are seeded on top of the collagen matrix scaffold and invade for 72 h at 37 °C, 95% humidity and 5% CO_2. (B) and (C) Average percentage of invasive MDCK cells treated with control siRNA (siCTR) or PKHD1 (siPKHD1) and their invasion depth. Percentage of invasive cells and invasion depth of siRNA (siPKHD1) treated cells is increased compared to control siRNA (siCTR) treated cells. (D) Invasion depth profile of invasive control siRNA (siCTR) and PKHD1 (siPKHD1) treated cells. Values are presented as median values with confidence interval of 95.46 %. A p-value below 0.0001 is considered as $***$ significant.

used to analyze the overall cellular deformability of MDCK cells, in which the fibrocystin gene PKHD1 has been specifically knocked down (siPKHD1 cells) or for control solely treated with control siRNA (siCTR cells). Since the PKHD1 knock-down is most effective 48–72 h after siRNA-mediated silencing of PKHD1, we investigated the effect of the fibrocystin function in MDCK epithelial cells on cellular mechanical properties, such as deformability in this timeframe. We used an optical cell stretcher device based on a dual beam laser trap to deform single suspended cells by optical induced surface forces. In briefly, we measured suspended cells as follows: cells are transported by the microfluidic system to the region of interest and trapped between two lasers with 'weak' laser powers of 100 mW for 1 s (trap phase). Trapped cells are than

deformed by increasing the laser powers in a step-like manner to 800 mW or 900 mW for 2 s (stretch phase). Laser powers are reduced to 100 mW for another 2 s during which the cell relaxation is recorded to reveal the cell behavior after external stress (relaxation phase). Finally, the complete cell deformation behavior parallel to the laser beam axis is monitored for a complete time interval of 5 s. Since every cell population underlies a broad viability, we performed large scale analysis measurements with relatively high-throughput (250 cells per hour) compared to conventional atomic force microscopic based mechanical analysis of bulk cellular properties (30 cells per hour). Hence, we analyzed a high number of cells for siRNA-mediated silencing of PKHD1 (siPKHD1) and control siRNA (siCTR) treatment. More precisely, we analyzed in total 2491 and 973 cells of siRNA PKHD1 treated cells and 2616 and 1044 cells for control siRNA treated cells for laser powers of 800 mW and 900 mW, respectively. We performed at least three different experiments for siPKHD1 and siCTR cells.

The deformation behavior of the cell axis parallel to the laser beam axis was observed over a time interval of 2 s and cells show a time-dependent creep behavior $J(t)$ (figures 2(A) and (B)). This creep behavior is defined as follows: $J(t) = \mathcal{E}(t)/\sigma_0$ where $\mathcal{E}(t) = [d(t) - d(0)]/d(0)$ is relative deformation of the cell along the laser beam axis and σ_0 is the optical induced stress, which depends linearly on the stretch laser power (Guck *et al* 2000, 2005). The creep dependent deformation, $J(t)$, was used to compare the mechanical deformability of both cell types. The siPKHD1 cells display an increased cellular deformability of their long axis, parallel to laser beam axis, compared to siCTR cells for 800 mW (figure 2(A)). Similar results were observed for a stretch laser power of 900 mW, siPKHD1 cells are obviously more deformable than siCTR cells (figure 2(B)). Furthermore, the median creep deformation at the end of the stretch curve was used to determine creep deformation at J ($t = 3$ s) to compare mechanical deformability, representing maximal deformation of the cell (see figure S1 (stacks.iop.org/PhysBio/16/066006/mmedia)). These results show that the maximal deformation is significantly increased for siPKHD1 cells with a maximal deformation of 3.254% ± 0.143% compared to siCTR cells with a maximal deformation of 2.943% ± 0.144% (p value < 0.0001, figure S1). Similar results were observed for a stretch laser power of 900 mW, siPKHD1 cells show a significantly increased maximal deformation of 3.839% ± 0.239% compared to siCTR cells with a maximal deformation of 3.199% ± 0.229% (p value < 0.0001, figure S1). These findings indicate that the fibrocystin gene PKHD1 regulates cellular deformability, since the cell softening behavior is associated with the loss of PKHD1 gene expression in MDCK cells.

The deformation behavior of the cell axis perpendicular to the laser light beam (termed perpendicular axis) shows also a creep behavior (figures 2(C) and (D)). The behaviors of these perpendicular cell axes are relatively equal for the stretch laser power of 800 mW applied to both cell types (figure 2(C)), while the perpendicular axis is increased in siPKHD1 cells compared to the perpendicular axis of siCTR cells for the stretch laser power of 900 mW (figure 2(D)). The median creep deformation at the end of the constriction curve of the perpendicular axis was utilized to determine the creep deformation of this axis at J ($t = 3$ s) to compare the mechanical deformability representing maximal constriction of the cell (figures 2(C) and (D)). There is no significant difference between the two cell types at the stretch laser power of 800 mW, whereas at the 900 mW stretch laser power, the constriction of the siPKHD1 cells −1.495% ± 0.174% is pronouncedly increased compared to siCTR cells −0.997% ± 0.179% (p value < 0.0001) (figure 2(D)).

The relaxation behavior of mechanically stressed cells is affected by knockdown of PKHD1 gene encoding fibrocystin

We assume a Kelvin–Voigt model with an elastic spring parallel to a viscous damper that properly fits our measured data during the stress application phase (Kunschmann *et al* 2017). In detail, a viscoelastic cell behaves as follows: when a stress is exerted on a cell, it deforms (viscous part) and relaxes upon stress removal due to its elastic part, while the viscous part of the cell maintains a partially deformed cell state (Wottawah *et al* 2005). The relaxation phase can be described more accurately with a Maxwell model with an elastic spring and a viscous damper in series or a Zener model, where an elastic spring and a viscous damper placed in parallel are both positioned in series to another elastic spring. During optical stretcher experiments the relaxation behavior of the cells was observed for 2 s directly after stress application (stretch phase). Although relaxation curves (same data as in figures 2(A) and (B), but the relaxation start of the major axis is set to the same starting point) exhibit a similar shape for both cell types at low laser power of 800 mW (figure 2(E)), for a higher stress exposure (at 900 mW laser power) siPKHD1 cells showed increased relaxation compared to siCTR cells (figure 2(F)). The relaxation behavior of the siPKHD1 cells and siCTR cells are not largely different. Hence, we cannot conclude that the fibrocystin gene PKHD1 alters the relaxation behavior of the major cell axis (parallel to laser beam axis). In contrast, the relaxation of perpendicular cells axis (minor cell axis) revealed different behaviors for both cell types (figures 2(C), (D), (G) and (H), same data as in 2(C) and (D), but the relaxation start is set to the same starting point). In detail, for both laser powers siPKHD1 cells responded with a reduced relaxation behavior of their minor cell axis compared to siCTR cells (figures 2(G) and (H)). In summary, these results indicate that the knockdown of the fibrocystin gene PKHD1 influences cell´s cytoskeleton in a manner that

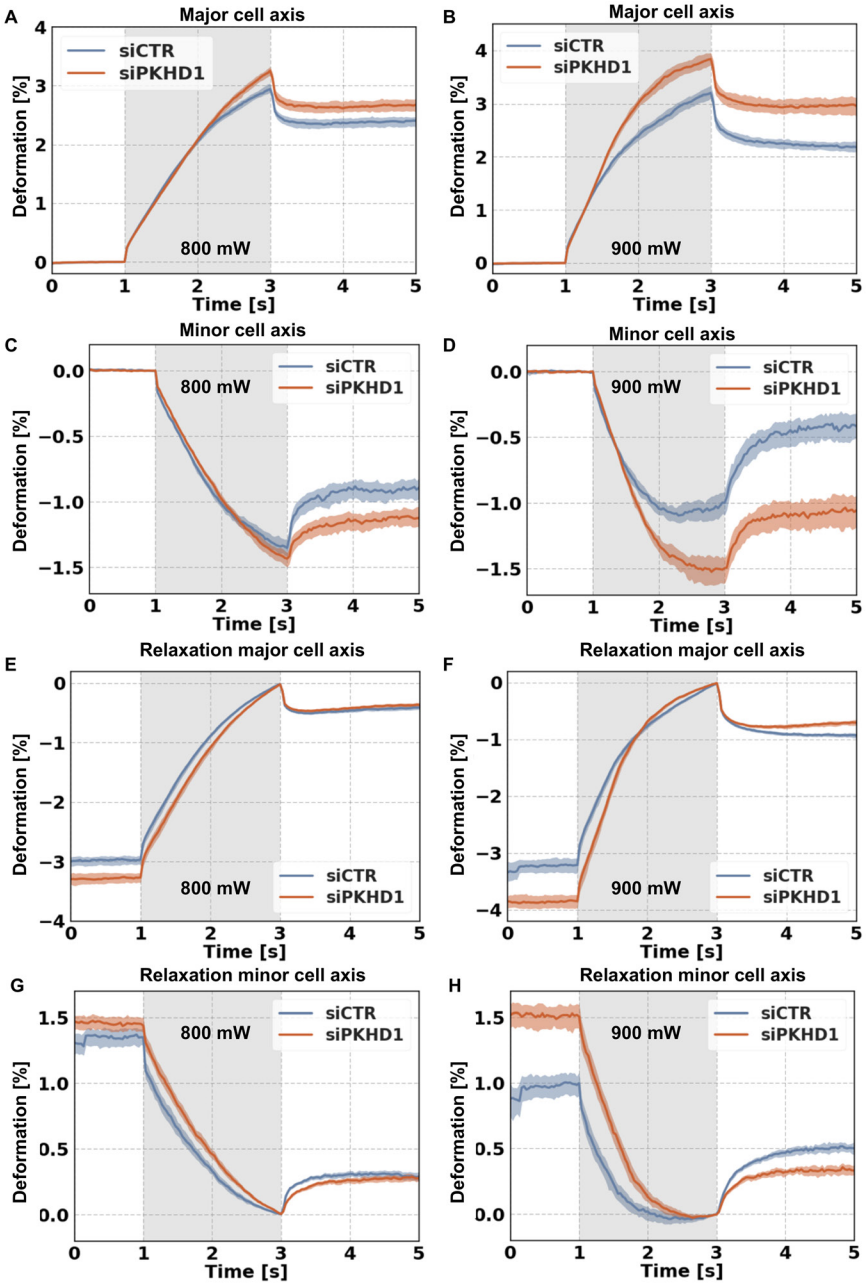

Figure 2. Mechanical properties such as cellular deformability of MDCK cells treated with control siRNA (siCTR) or specific PKHD1 siRNA (siPKHD1) using an optical stretcher. Cells are trapped in the first second at 100 mW laser power and then stretched at their major cell axis (parallel to laser beam axis) for 2 s by increasing laser power up to 800 mW (A) or 900 mW (B) along the laser beam axis. After stretching process, laser power is reduced to 100 mW and viscoelastic relaxation is observed for another 2 s. Mechanical constriction of siCTR and specific PKHD1 siRNA (siPKHD1) treated cells along their minor cell axis at laser powers of 800 mW (C) and 900 mW (D). Major cell axis relaxation behavior of siCTR and siPKHD1 treated MDCK cells parallel to the laser beam axis that is normalized on maximal deformation at laser powers of 800 mW (E) and 900 mW (F). Minor cell axis relaxation behavior of siCTR and siPKHD1 treated cells perpendicular to laser beam axis that is normalized on maximal deformation at laser powers of 800 mW (G) and 900 mW (H). (A)–(H) Data are presented as median values with confidence interval (2 ∗ SD) of 95.46%.

relaxation behavior of the minor cell axis was impaired after stress application.

Knockdown of PKHD1 gene encoding fibrocystin decreased cell–matrix adhesion forces

We performed cell–matrix adhesion force measurements with adhesive cells to investigate the effect of siRNA-mediated silencing of PKHD1 on the extracellular matrix adhesion using atomic force microscopy. Therefore, a flat cantilever coated with the extracellular matrix protein fibronectin was pressed on single adhesive cells with a force of 0.5 nN for a time point of 30 s (figure 3(A)). The force required to retract the cantilever from the cell is represented as the maximal adhesion force (figure 3(B)). In total, we analyzed 8 cells of siPKHD1 cells and 11 cells of control siCTR cells. The cell–matrix adhesion of siPKHD1 cells is decreased compared to siCTR cells (figure 3(B)), since the number of tethers (synonymously number of tubes) (figures 3(C) and S2) and the separation

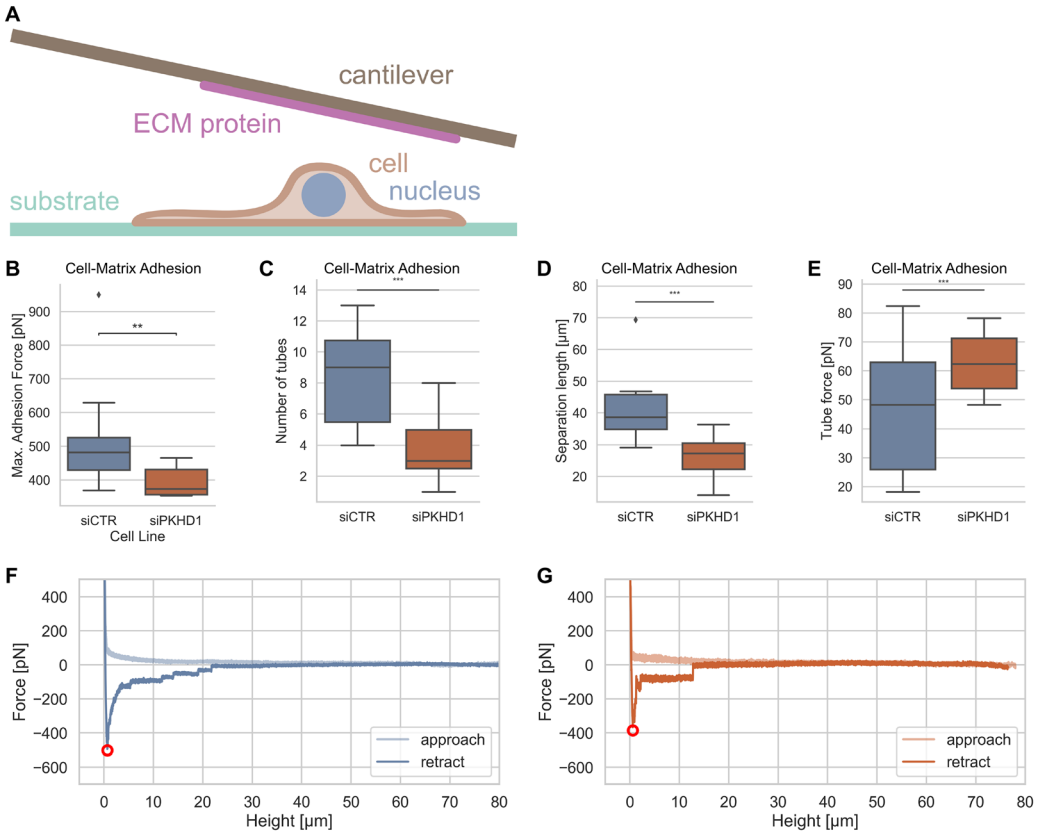

Figure 3. Cell–matrix adhesion forces of MDCK cells treated with control siRNA (siCTR) or PKHD1 (siPKHD1) using an atomic force microscope. (A) Schematic illustration of a flat cantilever pressing on an adhesive cell with a strength of 0.5 nN and a contact time of 30 s. (B) Maximal adhesion force of specific PKHD1 siRNA treated cells (siPKHD1 cells, $n = 8$) is significantly reduced compared to control siRNA treated cells (siCTR cells, $n = 11$). (C) Number of tubes, (D) Tube separation length and (E) Tube force of siPKHD1 and siCTR cells. Representative height curves of cell–matrix adhesion of control siRNA (siCTR) (F) or PKHD1 (siPKHD1) (G) treated cells with a force of 0.5 nN and contact time of 30 s. A p-value below 0.001 is considered as ∗∗ significant and a value below 0.0001 is considered as ∗∗∗ significant.

length (figure 3(D)) were significantly reduced. However, the tube force was reduced in siPKHD1 cells compared to siCTR cells (figure 3(E)). Representative retraction curves for both cell types, such as siCTR and siPKHD1, are provided shown in figures 3(F) and (G), respectively. In addition, the number of steps required for total cell–matrix adhesion was lower in siPKHD1 cells compared to siCTR cells (figures 3(G) and (H)). All these results demonstrate that the cell–matrix adhesion strength was decreased in PKHD1 knockdown cells compared to control cells, whereas the force of a single tube was increased in siPKHD1 cells compared to siCTR cells. Hence, it can however be concluded that PKHD1 regulates the cell–matrix adhesion.

Decreased cell–cell adhesion forces are detected after knockdown of PKHD1 gene encoding fibrocystin

Other studies have hypothesized and shown a relationship between cell–cell adhesion forces (Collins and Nelson 2015, Sander *et al* 1998, Maretzky *et al* 2005) and the migration ability into 3D extracellular matrices. Therefore, we hypothesized that the PKHD1 encoded fibrocystin influences the motility through altered cell–cell adhesion. Thus, we investigated whether the increased 3D motility of siPKHD1 cells compared to siCTR cells is associated with altered cell–cell adhesion forces. More precisely, we performed cell–cell adhesion force measurements to investigate the effect of siRNA-mediated silencing of PKHD1 on intercellular adhesion forces using atomic force microscopy. Therefore, a single suspended cell is attached to a flat fibronectin-coated cantilever and was pressed on an adherent cell of same cell type with a force of 0.5 nN for a time point of 30 s (figure 4(A)). During the retraction of the cantilever, the force required to tear both cells apart was determined. We analyzed in total 29 cells of siPKHD1 cells and 42 cells for siCTR cells. The siPKHD1 cells showed significantly decreased cell–cell adhesion forces compared to siCTR cells (figure 4(B)). In more detail, the cell–matrix force analysis revealed that the maximal adhesion force, number of tubes (figure 4(C)) and the tube separation length were all significantly decreased in siPKHD1 cells compared to control cells (figure 4(D)). In contrast, tube forces of the two cell types were not different (figure 4(E)). Representative retraction curves for both cell types including the tether rupture events are provided in figures 4(F) and (G). These results demonstrate that

siRNA-mediated silencing of PKHD1 contributes less to the cell–cell adhesion strength including decreased tether events. Finally, we have shown that decreased cell–cell adhesion forces are associated with increased capacity of PKHD1 knockdown cells to migrate into and through biomimetic 3D matrices such as collagen fiber matrices.

Discussion

Cell mobility in organ formation in embryogenesis and tissue homeostasis is a highly complex event and appears to be mainly dependent on biochemical and mechanical properties (Diz-Munoz *et al* 2010). At the same time, the cell requires precisely regulated dynamic interactions with the surrounding extracellular matrix environment (Van Helvert *et al* 2018, Charras and Sahai 2014). In turn, mechanical properties of cells are altered by their surrounding environment, including structural proteins and embedded cells (Mierke 2011a, 2011b, 2019). More specifically, the cell symmetry, known to be affected by fibrocystin (Kolb and Nauli 2008), affects the mechanical properties of cells, which in turn hinder organ development. However, the impact of fibrocystin on cell mechanics is still elusive.

Since it has been hypothesized that alterations of the cell mechanical properties, such as contractility, impact cellular functions, including migration and invasion, (Mierke *et al* 2008b, 2011, Pandya *et al* 2017, Wang *et al* 2019), we analyzed here the effect of fibrocystin on cell mechanics. In detail, cell contractility and low membrane-cortex interaction can induce a specific type of migration blebbing-driven migration (Diz-Munoz *et al* 2010). Hence, we investigated whether cellular mechanical properties such as cellular deformability, cell–cell and cell–matrix adhesion forces and migratory capacity of cells into 3D microenvironments are regulated by the fibrocystin gene PKHD1. In line with this hypothesis, it has been shown that the inhibition of actomyosin contractility with the myosin inhibitor blebbistatin restores positioning of centrosome and causes defects in cell morphogenesis in absence of the confinement (Pitaval *et al* 2010, Rodriguez-Fraticelli *et al* 2012). Mechanical properties of cells depend on the cell's actin cytoskeleton, whose organization have been shown to be regulated by fibrocystin (polycystin) (Yao *et al* 2014). In this blebbing migration mode the membrane cortex interaction is low compared to mesenchymal migration modes (Diz-Munoz *et al* 2010, Mierke 2015). In detail, the direction of cell movement can be determined by the interaction of fibrocystin, Pacsin 2 and the N-Wiskott–Aldrich syndrome protein (N-WASP) complex, which facilitates actin dynamics at the centrosome remodeling the membrane and shape of the nucleus (Yao *et al* 2014, Alekhina *et al* 2017). Moreover, it has been reported that fibrocystin increases the turnover of focal adhesions, which promotes the migration of cells (Castelli *et al* 2015, Fraine *et al* 2017). More precisely, fibrocystin promotes cell migration speed and the directionality of migration through the interaction with beta-catenin (Boca *et al* 2007).

The impact of fibrocystin encoding gene PKHD1 on cell mechanical properties, such as cellular deformability, cell–cell and cell–matrix adhesion forces, and its correlation with cell migration into 3D microenvironments is still not yet clearly defined. We investigated the invasiveness of siPKHD1 cells compared to siCTR control cells using a high throughput 3D invasion extracellular matrix assay. In detail, we used 3D collagen networks with a final concentration of 1.5 $g\,l^{-1}$ collagen and a depth of at least 500 μm. In fact, we found that the fibrocystin gene PKHD1 reduces the invasiveness indicating that it contributes to the non-invasive behavior of cells.

The major finding of this study is that cell mechanical properties, such as cellular deformability, facilitate the fibrocystin driven cell invasion into 3D extracellular matrices. Mechanical properties, such as adhesion forces, cellular deformability (compliance or inverse stiffness) and contractile and protrusive force generation and transmission play all an important role for invasion into dense 3D extracellular matrices (Guck *et al* 2005, Mierke *et al* 2008a, 2008b, Wolf *et al* 2013, Fischer *et al* 2017). In line with this, using the optical stretcher, we found that siPKHD1 cells were more deformable along their major cell axis compared to siCTR for both laser powers employed for the cell stretch. These results indicate that the membrane-cortex connection is weakened in fibrocystin knock-down cells. When the cell is stretched along its major axis, its minor axis, which is the axis perpendicular to the major cell axis and the laser beam axis, undergoes constriction. The constriction behavior can be seen significantly more pronounced in siPKHD1 cells compared to siCTR cells. Hence, this behavior also indicates that the membrane cortex connection is weakened in siPKHD1 cells. For both laser powers, siPKHD1 cells responded after cell stretching with a reduced deformation relaxation behavior compared to siCTR cells indicating that the cells are more viscous due to a loss of the membrane-cortex connection. There is still a residual deformation or equivalently a resting length change that has been found in MDCK cell monolayers after stress application (Khalilgharibi *et al* 2019). In summary, our results show that the knockdown of the fibrocystin gene PKHD1 is associated with increased cellular deformability in MDCK cells. These results are in agreement with several studies reporting that the invasiveness of specific cancer cell types is increased when the deformation is increased (Guck *et al* 2005, Remmerbach *et al* 2009, Runge *et al* 2014, Meinhövel *et al* 2018). However, the universality of this link between cell deformability (compliance or inverse stiffness) and invasion is still controversially discussed.

In order to probe with another biophysical technique, whether the increased deformability is associated with a reduced adhesion force, we found that

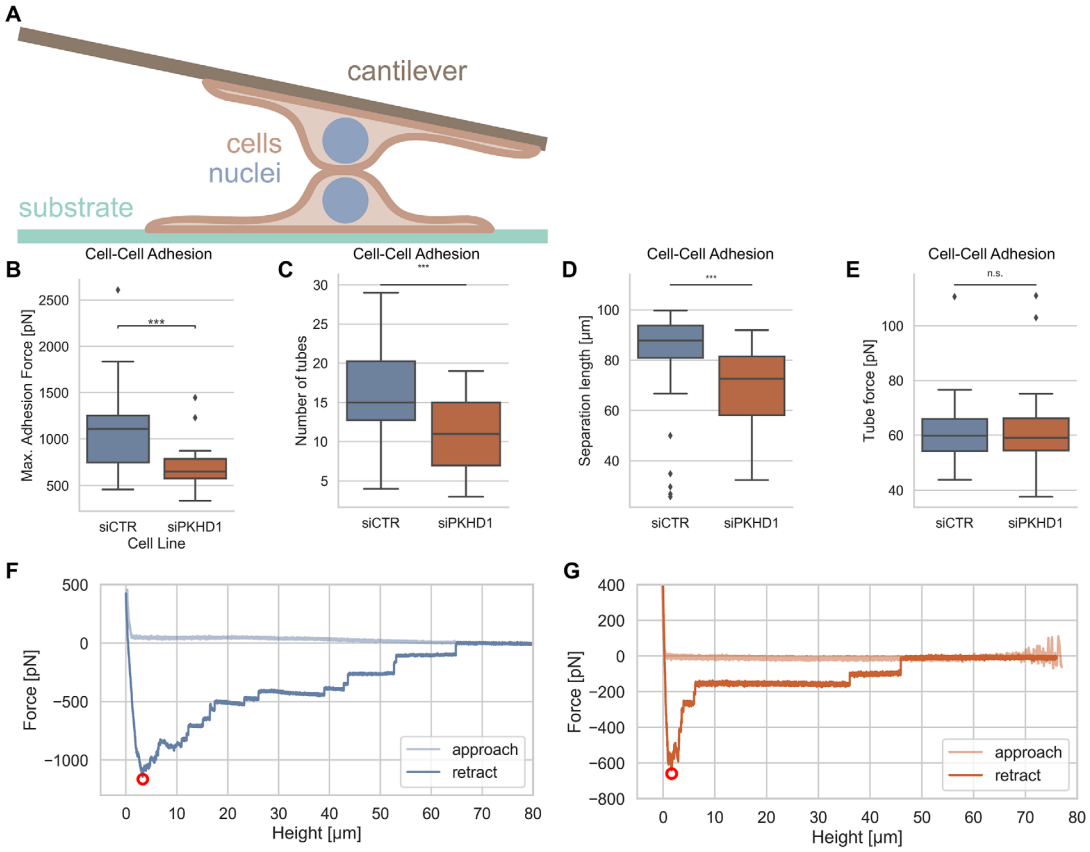

Figure 4. Cell–cell adhesion forces of MDCK cells treated with control siRNA (siCTR) or PKHD1 (siPKHD1) using an atomic force microscope. (A) Schematic illustration of an AFM measurement using a flat cantilever carrying a cell and pressing on an adherent cell of the same cell type with a strength of 0.5 nN and a contact time of 30 s. (B) Maximal adhesion force between two cells of same cell type of control siRNA (siCTR) and PKHD1 (siPKHD1) treated cells. Specific PKHD1 siRNA treated cells (siPKHD1 cells, $n = 29$) show a significantly reduced adhesion strength compared to control siRNA treated cells (siCTR cells, $n = 42$). (C) Number of tubes, (D) Tube separation length and (E) Tube force of siPKHD1 and siCTR cells. Representative height curves of cell–cell adhesion of control siRNA (siCTR) (F) or PKHD1 (siPKHD1) (G) treated cells with a force of 0.5 nN and contact time of 30 s. A p-value below 0.0001 is considered as *** significant.

atomic force microscopy-based cell–matrix adhesion forces of adhesive siPKHD1 cells and cell–cell adhesion forces of adhesive siPKHD1 cells are decreased compared to siCTR cells. However, since the membrane-cortex connection of cell–matrix and cell–cell adhesion receptors seems to be different. The retraction curves showed significant rupture events that are indicated by the small rupture steps (tethers or tubes). Moreover, siPKHD1 cells displayed decreased rupture events for both cell–matrix and cell–cell adhesion measurements. However, the tube force in siCTR cells is decreased compared to siPKHD1 cells indicating that the number of tubes contributes to the increased cell–matrix adhesion force of siCTR cells. The results show that the cell–matrix receptors are engaged with the integrin-ligand fibronectin coated to the cantilevers used for AFM probing. However, when the cell–cell adhesion forces were determined the tube forces are similar between the two cell types indicating that the increased maximal cell–cell adhesion force depends on the increased number of tubes in siCTR compared to siPKHD1 cells.

Overall, these results are in line with reports that couple fibrocystin to cell–matrix and cell–cell adhesion receptors or the Wnt-signaling process, respectively (Kim *et al* 2016, Fraine *et al* 2017). These findings suggest that all biophysical features, such as increased cellular deformability, decreased cell–matrix and decreased cell–cell adhesion forces seem to contribute to a high invasive phenotype of siPKHD1 cells. In detail, the weakening of cell-matrix and cell–cell adhesions enables the cells to invade into 3D matrix confinements more easily, without being hold back by strong cell–matrix adhesions or cell–cell adhesions.

In fact, we demonstrated that PKHD1 knockdown (siPKHD1) cells showed increased cellular deformability, increased constriction and increased invasiveness into confined 3D extracellular matrices compared to control siRNA (siCTR) treated cells. All these findings support the view that cell migration and invasion is favored, when the membrane cortex connection is decreased and the contractility (constriction) is increased. Hence, a migration type similar to a blebbing-migration phenotype seems to be chosen by siPKHD1 cells. More precisely, these siPKHD1 possess a weakened connection between the membrane and the cortex and we hypothesize that in these cells the connection of fibrocystin to the actin cytoskeleton via fil-

amin A, N-WASP or beta-catenin is reduced. Moreover, when this connection is decreased, the mechanotransduction signaling is also altered, which then affects the migration mode and migration capacity.

Our findings suggest that increased cellular deformability, decreased cell–cell and cell–matrix adhesion forces are responsible for the increased invasion of siPKHD1 cells into and through dense 3D extracellular matrices. Finally, these findings indicate that the fibrocystin encoding gene PKHD1 plays a central role as a biomarker for the disease. Finally, the mechanical phenotype of the cells may also serve as a marker for the disease.

Key findings (impact on science)

- The fibrocystin knockdown cells are more motile and invade increased and deeper in 3D extracellular matrices.
- PKHD1 plays a role in regulating cell mechanics and subsequently cell invasion.
- Knockdown of the fibrocystin gene PKHD1 increases cell invasion and causes a softening of the cells.
- A decrease of cell–matrix and cell–cell adhesion forces occurs after the fibrocystin gene PKHD1 knockdown.

Methods

Cells and cell culture

Madin-Darby canine kidney epithelial cells (MDCK) were purchased from ATCC-LGC-Promochem (Wesel, Germany). Cells were cultured in low-glucose (1 g l^{-1}) DMEM supplemented with 10% FCS (low endotoxin, <0.1 EU ml^{-1}), 2 mM L-glutamine and 100 U ml^{-1} penicillin–streptomycin (Biochrom, Berlin, Germany). 80% confluent cells were used in passages 4–10. Cells are harvested at 80% confluency using a 0.125%/0.025% Trypsin/EDTA (Biochrom, Berlin, Germany) solution in PBS buffer. All chemicals are obtained from Sigma (Taufkirchen, Germany) unless otherwise indicated.

Transient knockdown of PKHD1

MDCK cells were passaged two to three days before nucleofection. For a transient knock-down of PKHD1 cells were washed twice with PBS and harvested with a Trypsin/EDTA solution in PBS buffer for 10 min. 1.5 Mio cells were centrifuged at 90 g for 10 min and cell pellet was resuspended with 100 μl Nucleofector Solution L (Amaxa Cell Line Nucleofection Kit, Lonza Biosciences, Basel, Switzerland). Subsequently, the cell suspension was combined with 300 pmol siRNA (control siRNA or PKHD1 specific siRNA for knockdown cells). Nucleofection was accomplished by a nucleofector device using Amaxa Nucleofection System II b (Lonza Biosciences, basel, Switzerland). Finally, the cell suspension was mixed with 500 μl culture medium, transferred into a T25 flask and cultured at 37 °C, 95% humidity and 5% CO_2 for 48 h. Knockdown is most effective 48–72 h after siRNA treatment and hence all experiments were performed after this time interval. Expression levels after 48 hours were quantified by qRT-PCR (QuantiTect SYBRGreen PCR Master Mix, Qiagen, Hilden, Germany).

3D extracellular matrix invasion assays

3D extracellular matrix invasion assays were performed by using a type I collagen mixture of rat tail (one part) and bovine skin (two parts). This special combination of the collagens types leads to a collagen fiber network containing collagen fibers and crosslinking points similar to human extracellular matrices of connective tissue (Paszek *et al* 2009, Fischer *et al* 2017, Kunschmann *et al* 2017, 2019, Mierke *et al* 2017). Using these 3D extracellular matrices, we investigated the motility of the MDCK cells treated either with control siRNA (siCTR) or with PKDH1 specific siRNA (siPKDH1).

Six-well plates with 1.5 mg ml^{-1} collagen consisting of 1/3 collagen R (4 mg ml^{-1} rat collagen type I, Serva, Heidelberg, Germany) and 2/3 collagen G (4 mg ml^{-1} bovine collagen type I, Biochrom, Berlin, Germany), dH_20 and 1M phosphate buffer were prepared. The phosphate buffer contains sodium dihydrogen phosphate and disodium dihydrogen phosphate with a pH value of 7.4 and an ionic strength of 0.7. All solutions were precooled and mixed on ice to avoid polymerization start. Each well of the six-well plate was filled with 1.2 ml of the 1.5 mg ml^{-1} collagen mixture and polymerized at 37 °C, 95% humidity and 5% CO_2 for two hours. Polymerized extracellular matrix scaffolds were rinsed three times with PBS buffer and incubated with 2 ml DMEM (1.0 g l^{-1} Glucose) supplemented with 10% FCS and 100 U ml^{-1} penicillin-streptomycin (Fischer *et al* 2017, Kunschmann *et al* 2017). 80% confluent cells were treated with Trypsin/EDTA solution in PBS buffer for 4 min for transfer to invasion assays. 50.000 cells per well were seeded on top of the extracellular matrix scaffolds and cultured for 72 h at 37 °C, 95% humidity and 5% CO_2. Invasive and non-invasive cells were fixed with 2.5% glutaraldehyde (Serva, Heidelberg, Germany) in PBS buffer and stained with 4 μg ml^{-1} Hoechst 33 342 dye dissolved in PBS and stored in PBS at 4 °C. Invasive cells can clearly be distinguished from non-invasive cells since the nuclei of the non-invasive cells coincide with the topmost collagen fibers. More precisely, the percentage of invasive cells was determined by the nuclei that were located below the cell-layer of non-invasive cells adhering on the top of the matrix scaffold. Percentage of non-invasive and invasive cells and their invasion depth were determined in 100 random fields of view. These 100 z-stacks were measured in 10 × 10 matrix in the middle of each well with a distance of 4 μm between the layers. The z-stacks were recorded with a

20× objective (DMI8000B, Leica, Wetzlar, Germany) and 0.55× c-mount adaptor (Leica) for a CCD camera (Orca-R2, Hamamatsu-Photonics, Munich, Germany).

Optical cell stretcher measurements

MDCK cells treated with control siRNA (siCTR) or with PKHD1 specific siRNA (siPKDH1) were passaged one day before measurement to 70% confluency in a T25 flask at 37 °C, 95% humidity and 5% CO_2 (see table 1 for primer sequences). Cells were harvested with a Trypsin/EDTA (0.125%/0.025%) solution in PBS buffer for 4 min and centrifuged at 125 g (770 rpm) for 5 min. The cell pellet was resuspended in 700 μl culture medium. The optical cell stretcher is a dual-beam laser trap with two coaxial optical fibers facing each other. These fibers emit divergent laser beams propagating in opposite directions. The setup consists of a microfluidic chip connected to microfluidic pump which transports single suspended cells to the two laser beams. The setup is placed on an inverted phase-contrast microscope (Zeiss Axio Observer.Z1, Zeiss, Oberkochen, Germany) and cell deformations were recorded with a CCD camera (Basler A622f, Basler Vision Technologies, Switzerland, Guck *et al* 2005, Lincoln *et al* 2007, Kunschmann *et al* 2017, 2019, Mierke *et al* 2017). Cells were trapped at a low laser power (100 mW) and then deformed in parallel to the laser axis by increasing the laser powers up to 800 mW or 900 mW (Guck *et al* 2001). In detail, the cells were trapped at 100 mW for 1 s (termed trap phase), stretched by increasing the laser powers to 800 mW or 900 mW in a step-like manner for 2 s (stretch phase) and finally the laser powers were reduced to 100 mW for another 2 s (relaxation phase). All measured cells exhibited a creep behavior as response to the deformation of the cells along the laser axis. Additionally, the behavior of the cells perpendicular to the laser axis was recorded and analyzed. The temperature was kept at 23 °C. A broad range of cells was measured during each experiment to ensure that the determined results are representative of the entire cell population and can be reproduced.

Cellular deformation data analysis

Relative cell deformations were determined using an automated subpixel edge detection algorithm implemented in MathLab (Math Works, Guck *et al* 2001, 2005). The algorithm uses feature tracking to correct small angle rotations of the trapped cells. Cells with irregular shape were excluded, as they may introduce rotations during deformation of the cell leading to 'false' deformation results. All remaining cells were analyzed with respect to their creep behavior $J(t) = \mathfrak{E}(t)/\sigma_0$ where $\mathfrak{E}(t) = [d(t) - d(0)]/d(0)$ is the relative deformation of the cell along the laser beam axis and σ_0 is the optical induced stress, which depends linearly on the stretch laser powers (Guck *et al* 2000, 2005). All maximum deformation values were presented as median because optical deformation of the cell follows a non-Gaussian distribution. The bootstrapping method was used to estimate a 95.46% confidence interval (2 ∗ SD) for all median values.

Table 1. Primer sequences.

Primer name	Primer sequence
Dog_Ubi_for	TCT TCG TGA AAA CCC TGA CC
Dog_Ubi_rev	CCT TCA CAT TCT CGA TGG TG
Dog_HPRT_for	GCT TGC TGG TGA AAA GGA C
Dog_HPRT_rev	TTA TAG TCA AGG GCA TAT CC
Dog_GAPDH for	AACATCATCCCT-GCTTCCAC
Dog_GAPDH rev	GACCACCTGGTC-CTCAGTGT
Dog_PKHD1_tm_for	TCTCTGGGT-CAAATTGGCACT
Dog_PKHD1_tm_rev	CAACAGCACACCA-GACAGCA
Dog_PKHD1_42/43_44 for	TGCACT-GCTAGTGGGTACAG
Dog_PKHD1_42/43_44 rev	CCCTCGGTGCCA-GAAATACT
Dog_PKHD1_exon17 for	CCCAGCAGGGG-GATGAGAAT
Dog_ PKHD1_exon17 rev	AGCTCCCTCTAC-CAGACACA

Cell–matrix and cell–cell adhesion force measurements using atomic force microscopy

Cell–matrix adhesion force measurements of adhesive cells

Cell–matrix adhesion forces of adhesive control siRNA treated cells (siCTR) and PKHD1 treated cells (siPKHD1) were determined with an atomic force microscope (AFM) using CellHesionR200 (JPK, Berlin, Germany). The glass block of the AFM was cleaned with dH_20 and 70% ethanol before all measurements. The spring constant of a flat tipless cantilever (Arrow-TL2-50, NanoWorld, Neuchatel, Switzerland) was determined in culture medium by using the thermal noise method. This method is based on free fluctuations of the cantilever and the spring constant (force constant 0.03 N m^{-1}) was obtained by fitting a Lorenz function to the respective peak of the frequency spectrum (usually the second peak) (Kunschmann *et al* 2017, Mierke *et al* 2017). The tipless cantilevers were first incubated overnight at 4 °C with 20 μg ml^{-1} fibronectin. 80% confluent cells were harvested with a Trypsin/EDTA (0.125%/0.025%) solution in PBS buffer for 4 min, and 5000–6000 cells were seeded into a 3.5 cm plastic culture dish. Cells were cultured for at least 30 min to ensure adherence to the dish surface and measured on a pre-heated stage at 37 °C and 5% CO_2 influx with AFM. The cantilever was pressed on individual adherent cells with a force

of 0.5 nN for 30 s. Approach and retraction force-distance curves were recorded. Experiments were repeated at least three times. With one cantilever three to five cells adhered on the culture dish surface can be measured. The JPK data processing software was used to determine the minimum of the retraction curve representing the maximum force, which is referred to as adhesion force of the cells. We determined the tether events as described (Smolyakov *et al* 2016) and discriminated them from simple jumps (see figure S2).

Cell–cell adhesion force measurements of adhesive cells
The AFM method was also used to determine cell–cell adhesion forces between two cell types. Flat tipless cantilevers were coated with 20 μg ml^{-1} fibronectin at 4 °C overnight and the spring individual constant was determined as described above. 80% confluent cells were harvested with a Trypsin/EDTA (0.125%/0.025%) solution in PBS buffer for 4 min and 5000–6000 cells were seeded into a 3.5 cm plastic culture dish. Directly after cell seeding, the fibronectin-coated cantilever was placed into the cell suspension to attach a cell towards the cantilever. The cell-carrying cantilever and the cell suspension were cultured on a pre-heated stage at 37 °C and 5% CO_2 influx for two hours to ensure cell surface receptor recovery and cell–matrix adhesion to the surface. After two hours adhesive cells were measured by pressing the cell-carrying cantilever with 0.5 nN on an adherent cell for 30 s and approach and retraction force-distance curves were recorded. A new cantilever with a new attached cell was used for all three to five measured cells and the experiments were repeated at least three times. The maximum adhesion between the two cells (one attached to the cantilever and one adhered to the surface of the culture dish) was estimated with the JPK data processing software, where tilt and offset were corrected and subsequently the minimum of the retraction curve was determined representing the maximum adhesion force.

Statistics

The data were expressed as mean values ± SD unless otherwise stated. For statistical analyses, a two-tailed Student's *t*-test was performed, when the values are normal distributed. A *p*-value below 0.01 was considered as statistically significant. For AFM measurements, a Wilcoxon–Mann–Whitney statistical analysis (Mann–Whitney *U* test) was performed that is a nonparametric test of the null hypothesis (no relationship between two measured phenomena) and does not require normal distribution.

Acknowledgments

We thank Birga Soetje and Wolfgang H Ziegler for providing the siRNA treated MDCK cells and Nils Wilharm for helping to measure the cells using the AFM. This work was supported by the DFG (MI1211/18-1 and INST268/357-1 FUGG) and the EFRE-SAB Scientific infrastructure (No. 100299919).

ORCID iDs

Tony Fischer https://orcid.org/0000-0001-9361-8886
Claudia Tanja Mierke https://orcid.org/0000-0002-6622-335X

References

Alekhina O, Burstein E and Billadeau D D 2017 Cellular functions of WASP family proteins at a glance *J. Cell Sci.* **130** 2235–41
Blanchoin L, Boujemaa-Paterski R, Sykes C and Plastino J 2014 Actin dynamics, architecture and mechanics in cell motility *Physiol. Rev.* **94** 235–63
Boca M, D'Amato L, Distefano G, Polishchuk R S, Germino G G and Boletta A 2007 Polycystin-1 induces cell migration by regulating phosphatidylinositol 3-kinase-dependent cytoskeletal rearrangements and GSK3β-dependent cell–cell mechanical adhesion *Mol. Biol. Cell* **18** 4050–61
Bryant D M and Mostov K E 2008 From cells to organs: building polarized tissue *Nat. Rev. Mol. Cell Biol.* **9** 887–901
Charras G and Sahai E 2014 Physical influences of the extracellular environment on cell migration *Nat. Rev. Mol. Cell Biol.* **15** 813–24
Castelli M, de Pascalis C, Distefano G, Ducano N, Oldani A, Lanzetti L and Boletta A 2015 Regulation of the microtubular cytoskeleton by polycystin-1 favors focal adhesions turnover to modulate cell adhesion and migration *BMC Cell Biol.* **16** 15
Collins C and Nelson W J 2015 Running with neighbors: coordinating cell migration and Cell–cell Adhesion *Curr. Opin. Cell Biol.* **36** 62–70
Diz-Munoz A, Krieg M, Bergert M, Ibarlucea-Benitez I, Muller D J, Paluch E and Heisenberg C-P 2010 Control of directed cell migration *in vivo* by membrane-to-cortex attachment *PLoS Biol.* **8** e1000544
Fischer T, Wilharm N, Hayn A and Mierke C T 2017 Matrix and cellular mechanical properties are the driving factors for facilitating human cancer cell motility into 3D engineered matrices *Converg. Sci. Phys. Oncol.* **3** 044003
Fraine S L, Patel A, Duprat F and Sharif-Naeini R 2017 Dynamic regulation of TREK1 gating by polycystin 2 via a filamin a-mediated cytoskeletal mechanism *Sci. Rep.* **7** 17403
Guck J, Ananthakrishnan R, Mahmood H, Moon T J, Cunningham C C and Käs J 2001 The optical stretcher: a novel laser tool to micromanipulate cells *Biophys. J.* **81** 767–84
Guck J, Ananthakrishnan R, Moon T J, Cunningham C C and Käs J 2000 Optical deformability of soft biological dielectrics *Phys. Rev. Lett.* **84** 5451–4
Guck J *et al* 2005 Optical deformability as an inherent cell marker for testing malignant transformation and metastatic competence *Biophys. J.* **88** 3689–3698
Khalilgharibi N *et al* 2019 Stress relaxation in epithelial monolayers is controlled by actomyosin *Nat. Phys.* **15** 839–47
Kim S *et al* 2016 The polycystin complex mediates Wnt/Ca^{2+} signalling *Nat. Cell Biol.* **18** 752–64
Kolb R J and Nauli S M 2008 Ciliary dysfunction in polycystic kidney disease: an emerging model with polarizing potential *Frontiers Biosci.* **13** 4451–66
Kulkarni A H, Chatterjee A, Kondaiah P and Gundiah N 2018 TGF-β induces changes in breast cancer cell deformability *Phys. Biol.* **15** 065005
Kunschmann T, Puder S, Fischer T, Perez J, Wilharm N and Mierke C T 2017 Integrin-linked kinase regulates cellular mechanics facilitating the motility in 3D extracellular matrices *BBA Mol. Cell Res.* **1864** 580–93

Kunschmann T, Puder S, Fischer T, Steffen A, Klemens R and Mierke C T 2019 The small GTPase Rac1 regulates cellular mechanical properties facilitating cell motility into 3D extracellular matrices *Sci. Rep.* **9** 7675

Limdi A, Pérez-Escudero A, Li A and Gore J 2018 Asymmetric migration decreases stability but increases resilience in a heterogeneous metapopulation *Nat. Commun.* **9** 2969

Lincoln B, Schinkinger S, Travis K, Wottawah F, Ebert S, Sauer F and Guck J 2007 Reconfigurable microfluidic integration of a dual-beam laser trap with biomedical applications *Biomed. Microdevices* **9** 703–10

Maretzky T, Reiss K, Ludwig A, Buchholz J, Scholz F, Proksch E, de Strooper B, Hartmann D and Saftig P 2005 ADAM10 mediates E-cadherin shedding and regulates epithelial cell–cell adhesion, migration, and β-catenin translocation *PNAS* **102** 9182–7

Meinhövel F, Stange R, Schnauß J, Sauer M, Käs J A and Remmerback T W 2018 Changing cell mechanics—a precondition for malignant transformation of oral squamous carcinoma cells *Converg. Sci. Phys. Oncol.* **4** 034001

Mierke C T 2013a The integrin alphav beta3 increases cellular stiffness and cytoskeletal remodeling dynamics to facilitate cancer cell invasion *New J. Phys.* **15** 015003

Mierke C T 2013b Physical break-down of the classical view on cancer cell invasion and metastasis *Eur. J. Cell Biol.* **92** 89–104

Mierke C T 2014 The fundamental role of mechanical properties in the progression of cancer disease and inflammation *Rep. Prog. Phys.* **77** 076602

Mierke C T 2015 Physical view on migration modes *Cell Adhes Migr.* **9** 367–79

Mierke C T 2019 The matrix environmental and cell mechanical properties regulate cell migration and contribute to the invasive phenotype of cancer cells *Rep. Prog. Phys.* **82** 064602

Mierke C T, Fischer T, Puder S, Kunschmann T, Soetje B and Ziegler W H 2017 Focal adhesion kinase activity is required for actomyosin contractility-based invasion of cells into dense 3D matrices *Sci Rep.* **7** 42780

Mierke C T, Frey B, Fellner M, Herrmann M and Fabry B 2011 Integrin $\alpha5\beta1$ facilitates cancer cell invasion through enhanced contractile forces *J Cell Sci.* **124** 369–83

Mierke C T, Rösel D, Fabry B and Brábek J 2008b Contractile forces in tumor cell migration *Eur. J. Cell Biol.* **87** 669–76

Mierke C T, Zitterbart D P, Kollmannsberger P, Raupach C, Schlötzer-Schrehardt U, Goecke T W, Behrens J and Fabry B 2008a Breakdown of the endothelial barrier function in tumor cell transmigration *Biophys J.* **94** 2832–46

Mierke C T 2011a Endothelial cell's biomechanical properties are regulated by invasive cancer cells *Mol. Biosyst.* **8** 1639–49

Mierke C T 2011b The biomechanical properties of 3d extracellular matrices and embedded cells regulate the invasiveness of cancer cells *Cell biochem. biophys.* **61** 217–36

Onuchic L F *et al* 2002 PKHD1, the polycystic kidney and hepatic disease 1 gene, encodes a novel large protein containing multiple immunoglobulin-like plexin-transcription-factor domains and parallel beta-helix 1 prepeats *Am. J. Hum. Genet.* **70** 1305–17

Pandya P, Orgaz J L and Sanz-Moreno V 2017 Actomyosin contractility and collective migration: may the force be with you *Curr. Opin. Cell Biol.* **48** 87–96

Paszek M J, Boettiger D, Weaver V M and Hammer D A 2009 Integrin clustering is driven by mechanical resistance from the glycocalyx and the substrate *PLoS Comput. Biol.* **5** e1000604

Pitaval A, Tseng Q, Bornens M and Thery M 2010 Cell shape and contractility regulate ciliogenesis in cell cycle-arrested cells *J. Cell Biol.* **191** 303–12

Remmerbach T W, Wottawah F, Dietrich J, Lincoln B, Wittekind C and Guck J 2009 Oral cancer diagnosis by mechanical phenotyping *Cancer Res.* **69** 1728–32

Rodriguez-Fraticelli A E, Auzan M, Alonso M A, Bornens M and Martin-Belmonte F 2012 Cell confinement controls centrosome positioning and lumen initiation during epithelial morphogenesis *J. Cell Biol.* **198** 1011–23

Runge J, Reichert T E, Fritsch A, Käs J, Bertolini J and Remmerbach T W 2014 Evaluation of single cell biomechanics as potential marker for oral squamous cell carcinomas: a pilot study *Oral Dis.* **20** e120–7

Sander E E, van Delft S, ten Klooster J P, Reid T, van der Kammen R A, Michiels F and Collard J G 1998 Matrix-dependent Tiam1/Rac signaling in epithelial cells promotes either cell–cell adhesion or cell migration and is regulated by phosphatidylinositol 3-Kinase *J. Cell Biol.* **143** 1385–98

Smolyakov G, Formosa-Dague C, Severac C, Duval R E and Dague E 2016 High speed indentation measures by FV, QI and QNM introduce a new understanding of bionanomechanical experiments *Micron.* **85** 8–14

Van Helvert S, Storm C and Friedl P 2018 Mechanoreciprocity in cell migration *Nat. Cell Biol.* **20** 8–20

Wang W Y, Davidson C D, Lin D and Baker B M 2019 Actomyosin contractility-dependent matrix stretch and recoil induces rapid cell migration *Nat. Commun.* **10** 1186

Watanabe T, Wang S, Noritake J, Sato K, Fukata M, Takefuji M, Nakagawa M, Izumi N, Akiyama T and Kaibuchi K 2014 Interaction with IQGAP1 links APC to Rac1, Cdc42, and actin filaments during cell polarization and migration *Dev. Cell* **7** 871–83

Wilson P D 2011 Apico-basal polarity in polycystic kidney disease epithelia *Biochim. Biophys. Acta* **1812** 1239–48

Wolf K, te Lindert M, Krause M, Alexander S, te Riet J, Willis A L, Hoffman R M, Figdor C G, Weiss S J and Friedl P 2013 Physical limits of cell migration: control by ECM space and nuclear deformation and tuning by proteolysis and traction force *J. Cell Biol.* **201** 1069–84

Wottawah F, Schinkinger S, Lincoln B, Ananthakrishnan R, Romeyke M, Guck J and Käs J 2005 Optical rheology of biological cells *Phys. Rev. Lett.* **94** 098103

Yao G, Su X, Nguyen V, Roberts K, Li X, Takakura A, Plomann M and Zhou J 2014 Polycystin-1 regulates actin cytoskeleton organization and directional cell migration through a novel PC1-Pacsin 2-N-Wasp complex *Hum Mol Genet.* **23** 2769–79